Differential Effect of Cholesterol and Its Biosynthetic Precursors on Membrane Dipole Potential

Sourav Haldar,[†] Ravi Kumar Kanaparthi,[‡] Anunay Samanta,[‡] and Amitabha Chattopadhyay[†]*
[†]Centre for Cellular and Molecular Biology, Council of Scientific and Industrial Research, Hyderabad, India; and [‡]School of Chemistry, University of Hyderabad, Hyderabad, India

ABSTRACT   Dipole potential is the potential difference within the membrane bilayer, which originates due to the nonrandom arrangement of lipid dipoles and water molecules at the membrane interface. Cholesterol, a representative sterol in higher eukaryotic membranes, is known to increase membrane dipole potential. In this work, we explored the effects of immediate (7-DHC and desmosterol) and evolutionary (ergosterol) precursors of cholesterol on membrane dipole potential, monitored by the dual wavelength ratiometric approach utilizing the probe di-8-ANEPPS. Our results show that the effect of these precursors on membrane dipole potential is very different from that observed with cholesterol, although the structural differences among them are subtle. These results assume relevance, since accumulation of cholesterol precursors due to defective cholesterol biosynthesis has been reported to result in several inherited metabolic disorders such as the Smith-Lemli-Opitz syndrome. Interestingly, cholesterol (and its precursors) has a negligible effect on dipole potential in polyunsaturated membranes. We interpret these results in terms of *noncanonical orientation* of cholesterol in these membranes. Our results constitute the first report on the effect of biosynthetic and evolutionary precursors of cholesterol on dipole potential, and imply that a subtle change in sterol structure can significantly alter the dipolar field at the membrane interface.

INTRODUCTION

Dipole potential is an important electrostatic property of biological membranes. It is the potential difference within the membrane bilayer and is a manifestation of the nonrandom arrangement (orientation) of electric dipoles of constituent lipid molecules and water dipoles at the membrane interface (1–5). Relative to transmembrane and surface potential, dipole potential has been less explored. Depending on the composition of the membrane, its magnitude can vary from 200 to 400 mV (3). Since dipole potential is operative over a relatively small distance within the membrane, this results in a very large electric field strength in the range of 10^8-10^9 Vm^{-1} within the membrane (1). Dipole potential plays an important role in membrane phenomena. For example, alteration in the dipole potential of the membrane has been shown to modulate the activity of integral membrane proteins such as Na$^+$/K$^+$-ATPase (6) and the ion channel gramicidin (7). Modulation of dipole potential has been reported to affect the membrane insertion and folding of model amphiphilic peptides such as p25 (the signal sequence of subunit IV of cytochrome *c* oxidase) (8) and simian immunodeficiency viral fusion peptide (9). In addition, dipole potential has been implicated to influence the solvent relaxation dynamics at the membrane interface (10). Change in dipole potential is also believed to be involved in the action of anesthetics (11). The magnitude of dipole potential depends on the composition of electric dipoles (constitutive or adsorbed) at the membrane interface.

Cholesterol is an essential lipid in higher eukaryotic cellular membranes and plays a vital role in membrane organization, dynamics, function, and sorting (12,13). It is often found distributed nonrandomly in domains in biological and model membranes (13–15). These domains (sometimes termed "lipid rafts" (16)) contribute to variable patchiness and thickness of the membrane (17). Many of these domains are believed to be important for the maintenance of membrane structure (organization) and function, although characterizing the spatiotemporal resolution of these domains has proven to be challenging (18,19). The concept of such specialized membrane domains gains relevance in biology, since important cellular functions, such as signal transduction (20) and the entry of pathogens (21,22), have been implicated to these putative domains.

Cholesterol is the end product of a complex, multistep (involving >20 enzyme-catalyzed reactions) and exceedingly fine-tuned sterol biosynthetic pathway that parallels sterol evolution (23). There are two major pathways for cholesterol biosynthesis, the Kandutsch-Russell (24) and Bloch (23) pathways. Konrad Bloch speculated that the sterol biosynthetic pathway parallels sterol evolution (the "Bloch hypothesis"). According to this hypothesis, cholesterol has been selected over a very long timescale of natural evolution for its ability to optimize certain physical properties of eukaryotic cell membranes with regard to biological functions (23). Cholesterol precursors should therefore have properties that gradually support cellular function of higher organisms as they progress along the pathway toward cholesterol. Defects in the cholesterol biosynthetic pathway have been identified with several inherited metabolic disorders (25). Comparative studies on

Editor: David Cafiso.

the structure-function relationship of cholesterol and its evolutionary precursors on membranes therefore assume relevance.

7-Dehydrocholesterol (7-DHC) and desmosterol represent immediate biosynthetic precursors of cholesterol in the Kandutsch-Russell and Bloch pathways, respectively. Although 7-DHC differs from cholesterol only in a double bond at the 7th position in the sterol ring, desmosterol differs from cholesterol only in a double bond at the 24th position in its flexible alkyl side chain (see Fig. 1). Interestingly, accumulation of either 7-DHC or desmosterol due to defective sterol biosynthesis has been shown to result in fatal neurological disorders (25). Ergosterol, on the other hand, is an important evolutionary precursor of cholesterol and is the major sterol present in lower eukaryotes such as protozoa, yeast, and fungi, and in insects such as *Drosophila* (23). The chemical structure of ergosterol differs from that of cholesterol in having two additional double bonds (at 7th and 22nd positions) and a methyl group at the 24th position of the side chain (see Fig. 1). Both structural features appear relatively late during ergosterol biosynthesis in

response to some specialized requirements related to the physiology of organisms containing ergosterol as the major sterol (23). We have previously monitored the comparative effects of cholesterol and its precursors (7-DHC, desmosterol, and ergosterol) on membrane organization and dynamics using sensitive fluorescent membrane probes (26–28).

Cholesterol is known to influence physical properties of membranes, for example, membrane thickness (29) and water penetration (30,31). It has recently been reported that cholesterol increases membrane dipole potential (32). This could be due to a direct influence of unique molecular attributes of cholesterol (such as the dipole moment) or through cholesterol induced changes in membrane organization (e.g., condensation of the lipid headgroup area and/or water penetration). It has been suggested that a combination of both effects is operative (32). To explore the relationship between membrane dipole potential and sterol molecular structure in a comprehensive manner, we have monitored the effect of immediate and evolutionary precursors of cholesterol (7-DHC, desmosterol, and ergosterol) on membrane dipole potential. These results assume relevance in the context of previous reports that accumulation of cholesterol precursors leads to severe pathological conditions. Our results show that cholesterol precursors have differential effects on membrane dipole potential. This differential effect could be due to difference in dipole moment, orientation (tilt angle), or extent of water penetration in the membrane. In addition, we show that cholesterol (or its precursors) has a negligible effect on dipole potential in polyunsaturated lipid membranes. We interpret these results in the light of *noncanonical orientation* of cholesterol in polyunsaturated lipid membranes (33).
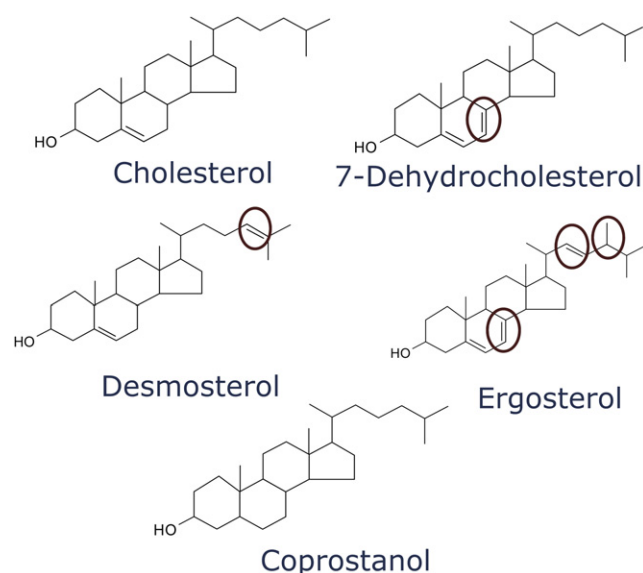

FIGURE 1   Molecular structures of sterols used. Cholesterol is an essential constituent of eukaryotic membranes and is the end product of the long and multi-step sterol biosynthetic pathway. The chemical structure of cholesterol is exceedingly fine-tuned by millions of years of evolution. 7-Dehydrocholesterol and desmosterol are immediate biosynthetic precursors of cholesterol in the Kandutsch-Russell (24) and Bloch (23) pathways, respectively. 7-Dehydrocholesterol differs with cholesterol only in a double bond at the 7th position in the sterol ring, and desmosterol differs with cholesterol only in a double bond at the 24th position in the flexible alkyl side chain (highlighted in their chemical structures). Ergosterol is the major sterol component present in lower eukaryotes such as yeast and fungi. The chemical structure of ergosterol differs from that of cholesterol in having two additional double bonds (at the 7th position in the sterol ring and the 22nd position in the side chain) and a methyl group at the 24th position of the side chain (highlighted). Coprostanol is a saturated sterol and is widely used as a biomarker.

MATERIALS AND METHODS

Dipole potential measurements

Dipole potential measurements were carried out by a dual-wavelength ratiometric approach using the voltage sensitive styrylpyridinium probe, 4-(2-(6-(dioctylamino)-2-naphthalenyl)ethenyl)-1-(3-sulfopropyl)-pyridinium inner salt (di-8-ANEPPS) (6,32,34,35). Steady-state fluorescence measurements were performed with a Hitachi (Tokyo, Japan) F-4010 spectrofluorometer using 1 cm path length quartz cuvettes. Excitation and emission slits with a nominal bandpass of 5 nm were used for all measurements. Background intensities of samples were subtracted from each sample to cancel any contribution due to the solvent Raman peak and other scattering artifacts. Steady state fluorescence intensities were recorded at two excitation wavelengths (420 and 520 nm). Emission wavelength was fixed at 670 nm. The fluorescence ratio (R), defined as the ratio of fluorescence intensity at an excitation wavelength of 420 nm to that at 520 nm (emission at 670 nm in both cases) was calculated (32). The choice of the emission wavelength (670 nm) at the red edge of the spectrum has previously been shown to rule out membrane fluidity effects (34). Dipole potential (ψ_d) in mV was calculated from R using the linear relationship (6,32)

$$\psi_d = \frac{(R + 0.3)}{(4.3 \times 10^{-3})}. \tag{1}$$

Dipole moment calculation

The ground state geometries of the systems were optimized in the gas phase using hybrid density functional B3LYP at the 6-31G level (36). The ground state dipole moments and Mulliken atomic charge densities were subsequently calculated for the optimized geometries of the respective systems using a higher basis set, B3LYP/6-31+G*, with added polarization and diffuse functions. These calculations were performed using the Gaussian 03 package (37).

Details of materials, sample preparation, and depth measurements are provided in the Supporting Material.

RESULTS

The dual wavelength ratiometric technique using di-8-ANEPPS represents a convenient approach to monitor membrane dipole potential (32,34,35). In this work, we utilized the dual-wavelength ratiometric approach to monitor dipole potential in 1-palmitoyl-2-oleoyl-sn-glycero-3-phosphocholine (POPC) membranes in presence of cholesterol and its biosynthetic and evolutionary precursors. Although the membrane orientation of di-8-ANEPPS has been previously addressed (38), the exact localization of the fluorophore in the membrane bilayer is not known. We therefore monitored the depth of the fluorophore in di-8-ANEPPS using the parallax method (39), which would provide useful information about its membrane orientation.

Localization of di-8-ANEPPS in the membrane bilayer

Membrane penetration depth represents an important parameter in the context of membrane structure and organization (40,41). Knowledge of the precise depth of a membrane embedded group or molecule often helps define the conformation and topology of membrane probes and proteins. In addition, properties such as polarity, fluidity, segmental motion, ability to form hydrogen bonds, and extent of solvent penetration are known to vary in a depth-dependent manner in the membrane. To gain an overall understanding of the orientation and location of membrane-bound di-8-ANEPPS, the penetration depth of the fluorescent styrylpyridinium group of di-8-ANEPPS in 1,2-dioleoyl-sn-glycero-3-phosphocholine (DOPC) membranes was determined. The membrane penetration depth of the styrylpyridinium group in di-8-ANEPPS was calculated by the parallax method (39) using the equation

$$z_{cF} = L_{c1} + \left\{ \frac{\left[(-1/\pi C) \ln(F_1/F_2) - L_{21}^2 \right]}{2 L_{21}} \right\}, \quad (2)$$

where z_{cF} is the depth of the fluorophore from the center of the bilayer, L_{c1} is the distance of the center of the bilayer from the shallow quencher (1-palmitoyl-2-(5-doxyl) stearoyl-sn-glycero-3-PC (5-PC) in this case), L_{21} is the difference in depth between the two quenchers (i.e., the transverse distance between the shallow and deep

quenchers), and C is the two-dimensional quencher concentration in the plane of the membrane (molecules/$Å^2$). Here, F_1/F_2 is the ratio of F_1/F_o and F_2/F_o, in which F_1 and F_2 are the fluorescence intensities in the presence of the shallow quencher (1,2-dioleoyl-sn-glycero-3-phosphotempocholine or 5-PC) and the deep quencher (1-palmitoyl-2-(12-doxyl) stearoyl-sn-glycero-3-PC), respectively, both at the same quencher concentration (C); F_o is the fluorescence intensity in the absence of any quencher. All the bilayer parameters used were the same as described previously (for further details about these parameters, see Chattopadhyay and London (39)). Our results show that the depth of penetration of the fluorescent styrylpyridinium group, on the average, was ~12.2 Å from the center of the bilayer (see Table S1 in the Supporting Material and Fig. 2; in principle, this distance represents the distance between the center of the bilayer and the transition dipole of the styrylpyridinium group). This suggests that di-8-ANEPPS is localized at the interfacial region of the membrane. This experimentally determined location of di-8-ANEPPS is in agreement with its proposed interfacial localization in membranes (35,42). Interestingly, the localization is consistent with the reported insensitivity of di-8-ANEPPS to surface potential (35).

Effect of sterols on dipole potential in POPC membranes

The fluorescence ratio (R) of di-8-ANEPPS (a charge-transfer dye) is sensitive to change in the dipolar field at the membrane interface where the dye is localized (see above and Fig. 2) by a putative electrochromic mechanism (35). According to this mechanism, the spectral shift exhibited by a charge-transfer dye such as di-8-ANEPPS is related to the electric field strength. It has recently been shown that the fluorescence ratio (R) of di-8-ANEPPS is sensitive only to dipole potential and is independent of specific molecular interactions (43). The effect of sterols on the
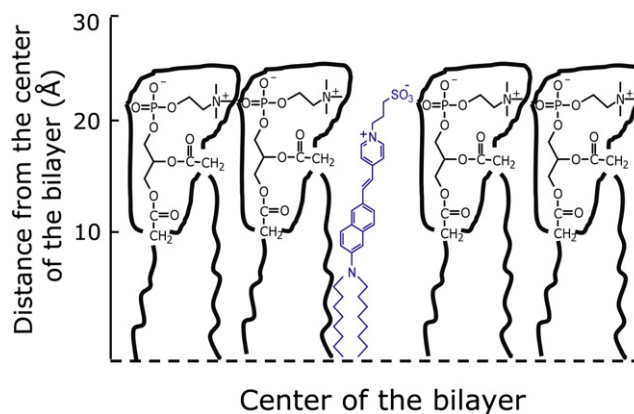

FIGURE 2 Schematic representation of one-half of the membrane bilayer showing the localization of di-8-ANEPPS in membranes. The horizontal line at the bottom indicates the center of the bilayer.

dipole potential of POPC membranes is shown in Fig. 3. The figure shows that the dipole potential of POPC membranes is ~363 mV. The membrane dipole potential exhibits progressive increase with increasing concentration of cholesterol and reaches a value of ~580 mV (i.e., increases by ~60%) in the presence of 40 mol % cholesterol. This is in agreement with results of earlier work, in which it was shown that cholesterol increases dipole potential in 1,2-dimyristoyl-sn-glycero-3-phosphocholine (DMPC) and 1,2-dioleoyl-sn-glycero-3-phosphocholine (DOPC) membranes in the fluid phase (32). To explore the relationship between membrane dipole potential and sterol structure, we explored the effect of biosynthetic and evolutionary precursors of cholesterol, such as 7-DHC, desmosterol, and ergosterol, on membrane dipole potential. Interestingly, the increase in dipole potential in the presence of these precursors is much less than in the presence of cholesterol. For example, the two immediate biosynthetic precursors of cholesterol, 7-DHC and desmosterol (differing from cholesterol only in a double bond; see Fig. 1), display increase in dipole potential up to ~430 mV at 40 mol % sterol concentration. This amounts to a relatively modest increase in dipole potential of ~18% in both cases (as opposed to ~60% in the case of cholesterol). The increase in dipole potential is even less (~8%) in the presence of 40 mol % ergosterol, reaching a value of ~391 mV. Ergosterol differs from cholesterol in having two additional double bonds and a methyl group (see Fig. 1). As a control, we monitored the effect of coprostanol (a saturated sterol with no double

bond, used as a biomarker) on dipole potential. The membrane dipole potential in the presence of 40 mol % coprostanol was ~411 mV (~13% increase). These results show that the ability of a sterol to modulate membrane dipole potential is varied and depends on its molecular structure. Even a subtle difference (such as a double bond) in the molecular structure of a sterol can give rise to a drastic difference in its ability to influence dipole potential.

The differential effect of these sterols on dipole potential merits some comment. It has been previously shown that these evolutionary precursors of cholesterol exert differential effects on membrane organization (26–28,44). Membrane dipole potential is related to dipole moment and dielectric constant of the medium according to the Helmholtz equation (1):

$$\psi_{d} = \frac{\mu_{\perp}}{A\ \varepsilon_0\ \varepsilon}, \qquad (3)$$

where ψ_{d} is the dipole potential, $\mu_{\perp}$ is the perpendicular component of the dipole moment (μ) along the bilayer normal, ε_0 is the permittivity in vacuum, ε is the dielectric constant, and A is the area/lipid molecule. According to Eq. 3, dipole potential should vary linearly with dipole moment and inversely with the effective molecular area and dielectric constant. The inverse relationship between dipole potential and effective molecular area has been previously demonstrated (45). Since dipole potential varies inversely with molecular area, the differential effect of sterols on dipole potential could be due to the difference in the condensing ability of these sterols. For example, the molecular area of a lipid molecule in the membrane bilayer is greater in the presence of 7-DHC (or desmosterol) relative to cholesterol (44,46). This implies that dipole density is less in the presence of 7-DHC (or desmosterol), which could lead to a reduction in dipole potential. The inverse dependence of dipole potential on dielectric constant can be further analyzed. We have recently shown that the vibronic peak intensity ratio (i.e., the ratio of the first and the third vibronic peak intensity, or I_1/I_3) of pyrene fluorescence emission can provide an estimate of dielectric constant (apparent polarity) in the interfacial region in model membranes (28), membrane-mimetic media such as micelles (47), and natural membranes (48). In addition, we showed that cholesterol reduces the dielectric constant of the membrane interface in model (28) and natural membranes (48). Interestingly, ergosterol (27), 7-DHC, and desmosterol (28) exhibit a reduction in dielectric constant. According to the Helmholtz equation, dipole potential should show a decrease with an increase in dielectric constant. The dependence of dipole potential on dielectric constant is shown in Fig. 4. The figure shows that dipole potential decreases more or less linearly with increase in dielectric constant in all cases. The difference in the slope of the lines in Fig. 4 could possibly be attributed to differential extents of water penetration induced by various sterols.
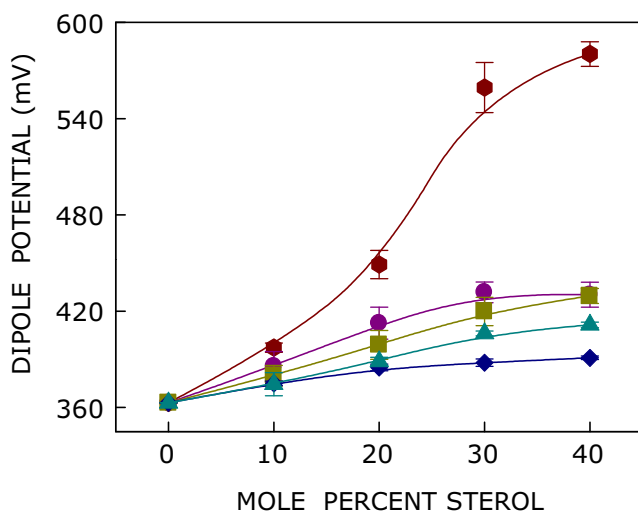

FIGURE 3 Effect of sterols on dipole potential of membranes. Dipole potential in POPC membranes as a function of increasing concentrations of cholesterol (●), 7-DHC (●), desmosterol (■), ergosterol (◆), and coprostanol (▲) are shown. Data points shown are means ± SE of at least three independent measurements. The ratio of di-8-ANEPPS to total lipid was 1:100 (mol/mol) and total lipid concentration was 0.43 mM. Measurements were carried out at room temperature (~23°C). Lines joining the data points are provided merely as viewing guides. See Materials and Methods and the Supporting Material for details.
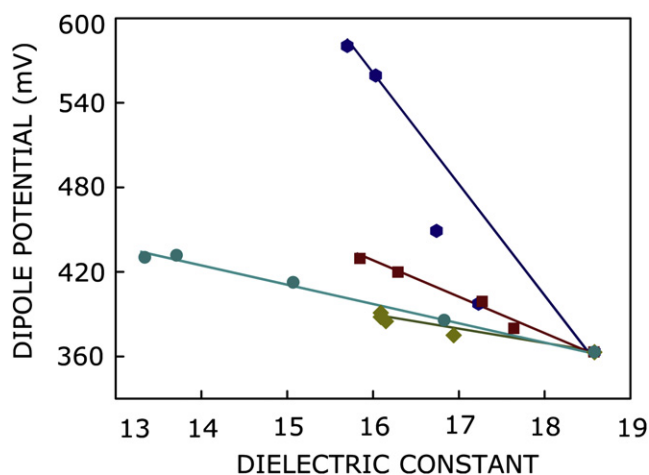
FIGURE 4   Validation of the Helmholtz relationship: dipole potential as a function of dielectric constant in the presence of cholesterol (●), 7-DHC (●), desmosterol (■), and ergosterol (◆). Sterol concentrations are the same as in Fig. 3 and ranged from 0 to 40 mol % (sterol concentration increases from left to right). Apparent dielectric constants were calculated from pyrene vibronic peak intensity ratio (I_1/I_3) (values for ergosterol/POPC membranes were taken from Shrivastava and Chattopadhyay (27), and those for cholesterol/POPC, 7-DHC/POPC, and desmosterol/POPC membranes from Shrivastava et al. (28)) using a calibration plot, (Dielectric constant (ε) = 0.0165(I_1/I_3) + 0.6565), previously described by one of us (48). The lines shown are linear fits. See text for more details.

Dipole moment calculations and dipole potential

To address the relationship between dipole moment and dipole potential, we carried out dipole moment calculations of sterols quantum mechanically (B3LYP/6-31G level, see Materials and Methods) (36). It was previously shown that the effect of cholesterol derivatives on membrane dipole potential correlates well with their dipole moment (32). The ground state electronic charge densities of the sterols used are shown in Fig. 5. Dipole moments calculated from these charge densities are shown in Table 1. According to the Helmholtz relationship (Eq. 3), increase in dipole potential in the presence of sterols varies linearly with dipole moment. The effective contribution of the dipole moment ($\mu_\perp$) of a given sterol in the membrane bilayer would depend on its orientation or tilt angle (θ) (44) with respect to the bilayer normal, given by

$$\mu_\perp = \mu \cos \theta. \qquad (4)$$

Table 1 shows the dipole moment and the perpendicular component of the dipole moment for sterols. A lower dipole potential in the case of membranes containing 7-DHC (or ergosterol) could possibly be due to the lower dipole moment of 7-DHC or ergosterol with respect to cholesterol. However, this does not appear to be true in the case of desmosterol and coprostanol, possibly implying that there could be other factors (such as the extent of water penetration and orientation of headgroup) influencing dipole potential.
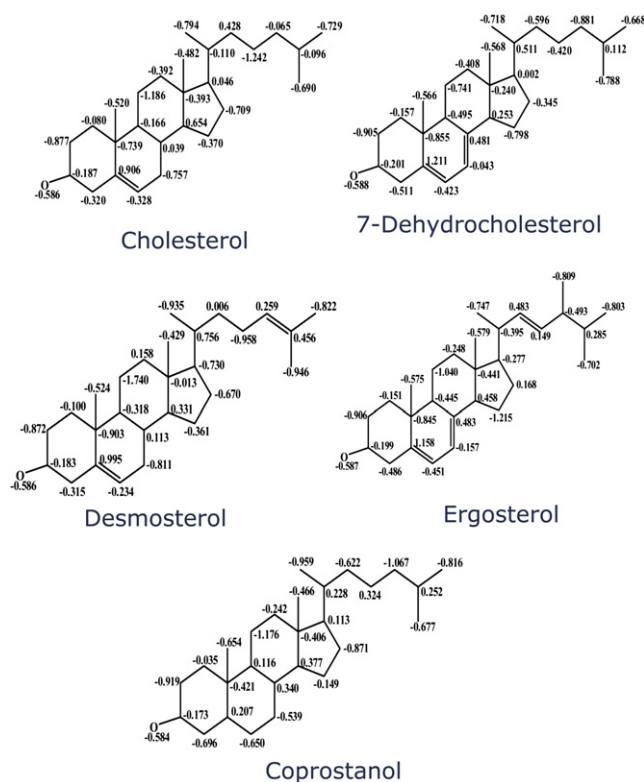

FIGURE 5   Ground state electronic charge densities of sterols. The charge densities were calculated using a density functional theory program. Charge-density calculations were performed using the Gaussian 03 program package. The chemical structures of sterols are shown in Fig. 1. See Materials and Methods for other details.

Effect of sterols on dipole potential in polyunsaturated membranes

The interaction between cholesterol and polyunsaturated lipids in membranes has recently gained considerable attention (33,49–52). Since cholesterol has a rigid tetracyclic ring in its structure, it displays poor affinity for polyunsaturated lipids due to their disordered nature (50). Interestingly, it has been shown recently that due to its aversion for polyunsaturated lipids (see Fig. 6), cholesterol resides flat (parallel to the membrane surface) in the middle of the membrane bilayer made of polyunsaturated 1,2-diarachidonoyl-*sn*-glycero-3-phosphocholine (DAPC) lipids (*noncanonical orientation*), as opposed to its upright *canonical orientation* in saturated lipid membranes (33,51,52). Since dipolar interaction is vectorial in nature, the interaction between membrane dipolar field and the molecular dipole of cholesterol is maximum in the canonical orientation. On the other hand, the interaction between membrane dipolar field and the molecular dipole of cholesterol is minimum in the noncanonical orientation in polyunsaturated membranes (Fig. 6).

The effect of sterols on the dipole potential of polyunsaturated DAPC membranes is shown in Fig. 7. DAPC membranes exhibit considerably lower dipole potential (~214 mV) relative to POPC membranes due to the presence

TABLE 1   Dipole moments and tilt angles of sterols

Sterol	Dipole moment (μ) (Debye)	Tilt angle* (°)	Perpendicular component of dipole moment ($\mu_{\perp}$)[†] (Debye)
Cholesterol	1.87	24.7	1.69
7-DHC	1.42	25.8	1.28
Desmosterol	2.08	24.9	1.87
Ergosterol	1.48	—	—
Coprostanol	2.03	—	—

*Tilt angles were taken from Røg et al. (44).

[†]Values were calculated using Eq. 4.

of eight *cis* double bonds (four in each acyl chain), in agreement with the finding that unsaturation in acyl chains reduces dipole potential (45). This could also be due to extensive disorder in the membrane induced by eight *cis* double bonds. Interestingly, increasing cholesterol content (up to 40 mol %) in the membrane shows very little effect on the dipole potential in DAPC membranes, in sharp
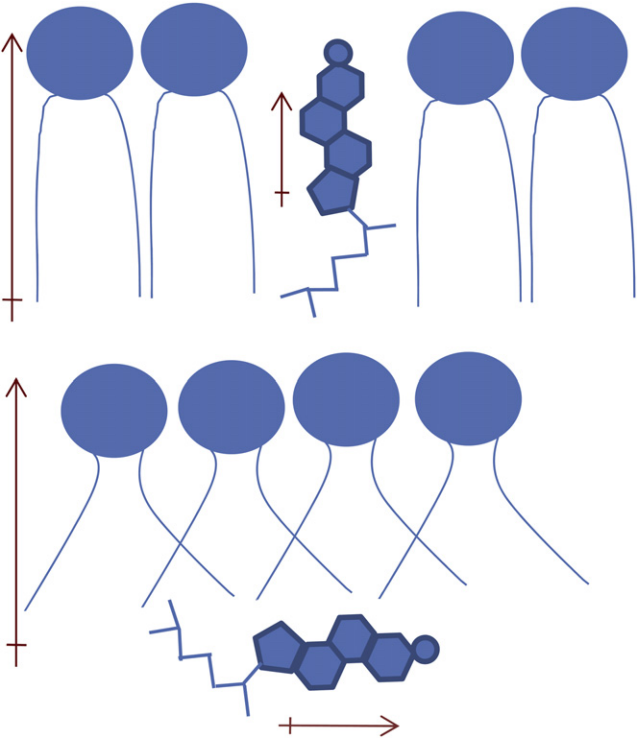
FIGURE 6   Different orientations of cholesterol in membranes composed of phospholipids with varying degrees of unsaturation. Cholesterol is orientated parallel to the membrane normal (perpendicular to the plane of the membrane) in membranes made of monounsaturated phospholipids such as POPC (*canonical orientation*). The interaction between the membrane dipolar field and the molecular dipole of cholesterol is maximum in the canonical orientation. Interestingly, cholesterol has been shown to reside in the middle of the bilayer in membranes composed of polyunsaturated phospholipids (such as DAPC) due to extreme disorder in these lipids (*noncanonical orientation*) (33,51). The interaction between the membrane dipolar field and the molecular dipole of cholesterol is minimum in this orientation. See text for more details.
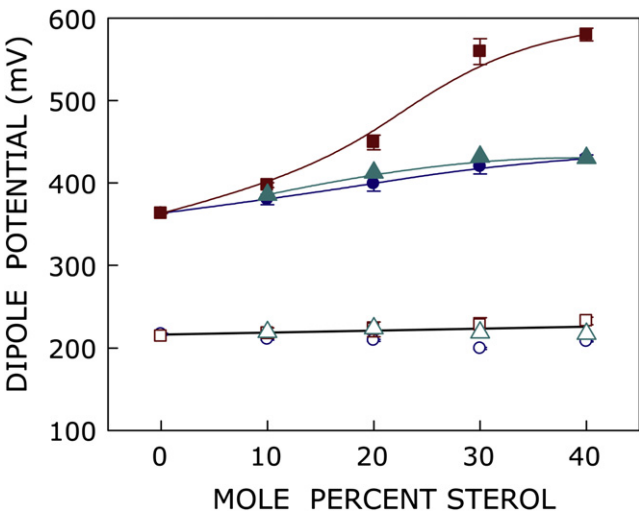
FIGURE 7   Invariance of dipole potential with sterol concentration in polyunsaturated (DAPC) membranes. Dipole potential in DAPC (*open symbols*) membranes is shown as a function of increasing concentrations of cholesterol ($\square$), 7-DHC ($\triangle$), and desmosterol ($\bigcirc$). Dipole potential values in monounsaturated (POPC) membranes at the same sterol concentrations (cholesterol ($\blacksquare$), 7-DHC ($\blacktriangle$), and desmosterol ($\bullet$)) are shown for comparison. Data points represent the mean $\pm$ SE of at least three independent measurements. The ratio of di-8-ANEPPS to total lipid was 1:100 (mol/mol) and total lipid concentration was 0.43 mM. Measurements were carried out at room temperature (~23°C). Lines joining the data points merely serve as viewing guides. See Materials and Methods and the Supporting Material for details.

contrast to observations in POPC membranes. Even 7-DHC and desmosterol are found not to influence membrane dipole potential in polyunsaturated DAPC membranes (see Fig. 7). These results suggest that the possible orientation of these sterols in the polyunsaturated membrane could be noncanonical (Fig. 6).

DISCUSSION

Structure-function relationship of cholesterol and its precursors (biosynthetic and evolutionary) in membranes represents a multidimensional problem that constitutes a crucial step in understanding the molecular basis of diseases caused by altered sterol biosynthesis. Dipole potential is a less explored, yet important, fundamental property of biological membranes. In this work, we explored the effect of immediate (7-DHC and desmosterol) and evolutionary (ergosterol) precursors of cholesterol on membrane dipole potential. We show that the effect of precursors of cholesterol such as 7-DHC, desmosterol, and ergosterol on membrane dipole potential is very different than that of cholesterol, despite subtle structural differences with cholesterol (Fig. 1). To the best of our knowledge, our results constitute the first report on the effect of biosynthetic and evolutionary precursors of cholesterol on dipole potential. The differential effect of cholesterol and its precursors on dipole potential could be attributed to a number of

factors, such as dipole moment, orientation (tilt angle), and condensing ability of these sterols. In addition, the differential effect on dipole potential could also be influenced by the extent of polarization of interfacial water by different sterols (32).

These results assume relevance in light of reports that accumulation of cholesterol precursors results in severe (often fatal) diseases (25,53). For example, accumulation of 7-DHC results in a neurological disorder called Smith-Lemli-Opitz Syndrome (SLOS) (54,55). SLOS is a congenital and developmental malformation syndrome associated with defective cholesterol biosynthesis. SLOS is caused by mutations in the gene encoding 3β-hydroxy-steroid-Δ^7-reductase, an enzyme required in the final step of the Kandutsch-Russell pathway of cholesterol biosynthesis. SLOS is clinically diagnosed by reduced plasma levels of cholesterol, along with elevated levels of 7-DHC (54–56). On the other hand, accumulation of desmosterol results in desmosterolosis (57), which is caused by mutations in the gene encoding 3β-hydroxy-steroid-Δ^{24}-reductase, an enzyme required in the ultimate step of the Bloch pathway of cholesterol biosynthesis. Desmosterolosis is clinically characterized by elevated levels of desmosterol accompanied by reduced levels of cholesterol (58).

Cholesterol is an exceedingly fine-tuned molecule, perfected over millions of years of evolution, to optimize its biological function. Previous studies have reported that structural features such as an intact alicyclic chain, a free 3β-OH group, a planar $\Delta5$ (6) double bond, angular methyl groups, and a branched 7-carbon alkyl chain at the 17β position (see Fig. 1), have all been found to be necessary for the complex biological function displayed by cholesterol (59–62). As a result, the function of membrane proteins, supported by cholesterol, is often not maintained even with close analogs of cholesterol. For example, it was earlier shown by one of us that 7-DHC and desmosterol cannot support the activity of the serotonin$_{1A}$ receptor (63–65), an important G-protein coupled receptor that requires membrane cholesterol for its function (66,67).

Our results show that biosynthetic and evolutionary precursors of cholesterol exhibit differential ability to modulate membrane dipole potential. It has been recently reported that various lipid headgroups contribute differentially to the membrane dipole potential, which could explain their different effects on the function of membrane proteins (68). It has been previously proposed that membrane microdomains (sometimes termed "lipid rafts") could influence membrane receptor activity by altering dipole potential (4,69,70). Spatial imaging of dipole potential (i.e., a dynamic map of dipole potential on the cell surface) as a result of signaling therefore represents an exciting possibility (69). In addition, our results with polyunsaturated membranes show that dipole potential is sensitive to the orientation of dipoles in the membrane. We therefore propose that interaction of the α-helix dipole (71) of proteins and peptides with the membrane dipolar field could be an important determinant in membrane physiology. Dipole potential measurements could therefore be utilized to monitor the orientation of proteins and peptides in membranes.

From a broader perspective, our results demonstrate that a small change in sterol structure can alter the dipolar field at the membrane interface considerably, which could have implications for pathogenicity associated with defective cholesterol biosynthesis. We envisage that evolution of sterols across various species helps to maintain specific electrostatic properties at membrane interfaces. We conclude that fine-tuning of the structure-function relationship in sterols constitutes a challenging problem, the study of which could provide insight into the molecular basis of diseases caused by altered sterol biosynthesis.

SUPPORTING MATERIAL

REFERENCES

1. Clarke, R. J. 2001. The dipole potential of phospholipid membranes and methods for its detection. *Adv. Colloid Interface Sci.* 89-90: 263–281.

2. Brockman, H. 1994. Dipole potential of lipid membranes. *Chem. Phys. Lipids.* 73:57–79.

3. Demchenko, A. P., and S. O. Yesylevskyy. 2009. Nanoscopic description of biomembrane electrostatics: results of molecular dynamics simulations and fluorescence probing. *Chem. Phys. Lipids.* 160:63–84.

4. O'Shea, P. 2005. Physical landscapes in biological membranes: physico-chemical terrains for spatio-temporal control of biomolecular interactions and behaviour. *Philos. Transact. A Math. Phys. Eng. Sci.* 363:575–588.

5. Zheng, C., and G. Vanderkooi. 1992. Molecular origin of the internal dipole potential in lipid bilayers: calculation of the electrostatic potential. *Biophys. J.* 63:935–941.

6. Starke-Peterkovic, T., N. Turner, …, R. J. Clarke. 2005. Electric field strength of membrane lipids from vertebrate species: membrane lipid composition and Na^+-K^+-ATPase molecular activity. *Am. J. Physiol. Regul. Integr. Comp. Physiol.* 288:R663–R670.

7. Duffin, R. L., M. P. Garrett, …, D. D. Busath. 2003. Modulation of lipid bilayer interfacial dipole potential by phloretin, RH421, and 6-ketocholestanol as probed by gramicidin channel conductance. *Langmuir.* 19:1439–1442.

8. Cladera, J., and P. O'Shea. 1998. Intramembrane molecular dipoles affect the membrane insertion and folding of a model amphiphilic peptide. *Biophys. J.* 74:2434–2442.

9. Cladera, J., I. Martin, …, P. O'Shea. 1999. Characterization of the sequence of interactions of the fusion domain of the simian immunodeficiency virus with membranes. Role of the membrane dipole potential. *J. Biol. Chem.* 274:29951–29959.

10. Mukherjee, S., and A. Chattopadhyay. 2005. Influence of ester and ether linkage in phospholipids on the environment and dynamics of the membrane interface: a wavelength-selective fluorescence approach. *Langmuir.* 21:287–293.

11. Cafiso, D. S. 1998. Dipole potentials and spontaneous curvature: membrane properties that could mediate anesthesia. *Toxicol. Lett.* 100-101:431–439.

12. Simons, K., and E. Ikonen. 2000. How cells handle cholesterol. *Science.* 290:1721–1726.

13. Mouritsen, O. G., and M. J. Zuckermann. 2004. What's so special about cholesterol? *Lipids.* 39:1101–1113.

14. Mukherjee, S., and F. R. Maxfield. 2004. Membrane domains. *Annu. Rev. Cell Dev. Biol.* 20:839–866.

15. Chaudhuri, A., and A. Chattopadhyay. 2011. Transbilayer organization of membrane cholesterol at low concentrations: implications in health and disease. *Biochim. Biophys. Acta.* 1808:19–25.

16. Lingwood, D., and K. Simons. 2010. Lipid rafts as a membrane-organizing principle. *Science.* 327:46–50.

17. Engelman, D. M. 2005. Membranes are more mosaic than fluid. *Nature.* 438:578–580.

18. Jacobson, K., O. G. Mouritsen, and R. G. W. Anderson. 2007. Lipid rafts: at a crossroad between cell biology and physics. *Nat. Cell Biol.* 9:7–14.

19. Ganguly, S., and A. Chattopadhyay. 2010. Cholesterol depletion mimics the effect of cytoskeletal destabilization on membrane dynamics of the serotonin$_{1A}$ receptor: a zFCS study. *Biophys. J.* 99:1397–1407.

20. Simons, K., and D. Toomre. 2000. Lipid rafts and signal transduction. *Nat. Rev. Mol. Cell Biol.* 1:31–39.

21. Riethmüller, J., A. Riehle, …, E. Gulbins. 2006. Membrane rafts in host-pathogen interactions. *Biochim. Biophys. Acta.* 1758:2139–2147.

22. Pucadyil, T. J., and A. Chattopadhyay. 2007. Cholesterol: a potential therapeutic target in *Leishmania* infection? *Trends Parasitol.* 23:49–53.

23. Bloch, K. E. 1983. Sterol structure and membrane function. *CRC Crit. Rev. Biochem.* 14:47–92.

24. Kandutsch, A. A., and A. E. Russell. 1960. Preputial gland tumor sterols. 3. A metabolic pathway from lanosterol to cholesterol. *J. Biol. Chem.* 235:2256–2261.

25. Porter, F. D., and G. E. Herman. 2011. Malformation syndromes caused by disorders of cholesterol synthesis. *J. Lipid Res.* 52:6–34.

26. Arora, A., H. Raghuraman, and A. Chattopadhyay. 2004. Influence of cholesterol and ergosterol on membrane dynamics: a fluorescence approach. *Biochem. Biophys. Res. Commun.* 318:920–926.

27. Shrivastava, S., and A. Chattopadhyay. 2007. Influence of cholesterol and ergosterol on membrane dynamics using different fluorescent reporter probes. *Biochem. Biophys. Res. Commun.* 356:705–710.

28. Shrivastava, S., Y. D. Paila, …, A. Chattopadhyay. 2008. Differential effects of cholesterol and its immediate biosynthetic precursors on membrane organization. *Biochemistry.* 47:5668–5677.

29. Nezil, F. A., and M. Bloom. 1992. Combined influence of cholesterol and synthetic amphiphilic peptides upon bilayer thickness in model membranes. *Biophys. J.* 61:1176–1183.

30. Simon, S. A., T. J. McIntosh, and R. Latorre. 1982. Influence of cholesterol on water penetration into bilayers. *Science.* 216:65–67.

31. Subczynski, W. K., A. Wisniewska, …, A. Kusumi. 1994. Hydrophobic barriers of lipid bilayer membranes formed by reduction of water penetration by alkyl chain unsaturation and cholesterol. *Biochemistry.* 33:7670–7681.

32. Starke-Peterkovic, T., N. Turner, …, R. J. Clarke. 2006. Cholesterol effect on the dipole potential of lipid membranes. *Biophys. J.* 90:4060–4070.

33. Harroun, T. A., J. Katsaras, and S. R. Wassall. 2008. Cholesterol is found to reside in the center of a polyunsaturated lipid membrane. *Biochemistry.* 47:7090–7096.

34. Clarke, R. J., and D. J. Kane. 1997. Optical detection of membrane dipole potential: avoidance of fluidity and dye-induced effects. *Biochim. Biophys. Acta.* 1323:223–239.

35. Gross, E., R. S. Bedlack, Jr., and L. M. Loew. 1994. Dual-wavelength ratiometric fluorescence measurement of the membrane dipole potential. *Biophys. J.* 67:208–216.

36. Lee, C., W. Yang, and R. G. Parr. 1988. Development of the Colle-Salvetti correlation-energy formula into a functional of the electron density. *Phys. Rev. B Condens. Matter.* 37:785–789.

37. Frisch, M. J., G. W. Trucks, …, J. A. Pople. 2004. Gaussian 03, Rev. C.02. Gaussian, Wallingford, CT.

38. Lambacher, A., and P. Fromherz. 2001. Orientation of hemicyanine dye in lipid membrane measured by fluorescence interferometry on a silicon chip. *J. Phys. Chem. B.* 105:343–346.

39. Chattopadhyay, A., and E. London. 1987. Parallax method for direct measurement of membrane penetration depth utilizing fluorescence quenching by spin-labeled phospholipids. *Biochemistry.* 26:39–45.

40. Chattopadhyay, A. 1992. Membrane penetration depth analysis using fluorescence quenching: a critical review. *In* Biomembrane Structure and Function: The State of the Art. B. P. Gaber and K. R. K. Easwaran, editors. Adenine Press, Schenectady, NY. 153–163.

41. London, E., and A. S. Ladokhin. 2002. Measuring the depth of amino acid residues in membrane-inserted peptides by fluorescence quenching. *In* Current Topics in Membranes. D. Benos and S. Simon, editors. Elsevier, San Diego, CA. 89–115.

42. Le Goff, G., M. F. Vitha, and R. J. Clarke. 2007. Orientational polarisability of lipid membrane surfaces. *Biochim. Biophys. Acta.* 1768:562–570.

43. Robinson, D., N. A. Besley, …, J. D. Hirst. 2011. Di-8-ANEPPS emission spectra in phospholipid/cholesterol membranes: a theoretical study. *J. Phys. Chem. B.* 115:4160–4167.

44. Róg, T., M. Pasenkiewicz-Gierula, …, M. Karttunen. 2009. Ordering effects of cholesterol and its analogues. *Biochim. Biophys. Acta.* 1788:97–121.

45. Clarke, R. J. 1997. Effect of lipid structure on the dipole potential of phosphatidylcholine bilayers. *Biochim. Biophys. Acta.* 1327:269–278.

46. Serfis, A. B., S. Brancato, and S. J. Fliesler. 2001. Comparative behavior of sterols in phosphatidylcholine-sterol monolayer films. *Biochim. Biophys. Acta.* 1511:341–348.

47. Chaudhuri, A., S. Haldar, and A. Chattopadhyay. 2009. Organization and dynamics in micellar structural transition monitored by pyrene fluorescence. *Biochem. Biophys. Res. Commun.* 390:728–732.

48. Saxena, R., S. Shrivastava, and A. Chattopadhyay. 2008. Exploring the organization and dynamics of hippocampal membranes utilizing pyrene fluorescence. *J. Phys. Chem. B.* 112:12134–12138.

49. Shaikh, S. R., and M. A. Edidin. 2006. Membranes are not just rafts. *Chem. Phys. Lipids.* 144:1–3.

50. Wassall, S. R., and W. Stillwell. 2009. Polyunsaturated fatty acid-cholesterol interactions: domain formation in membranes. *Biochim. Biophys. Acta.* 1788:24–32.

51. Harroun, T. A., J. Katsaras, and S. R. Wassall. 2006. Cholesterol hydroxyl group is found to reside in the center of a polyunsaturated lipid membrane. *Biochemistry.* 45:1227–1233.

52. Kucerka, N., D. Marquardt, …, J. Katsaras. 2009. The functional significance of lipid diversity: orientation of cholesterol in bilayers is determined by lipid species. *J. Am. Chem. Soc.* 131:16358–16359.

53. Waterham, H. R. 2006. Defects of cholesterol biosynthesis. *FEBS Lett.* 580:5442–5449.

54. Waterham, H. R., and R. J. A. Wanders. 2000. Biochemical and genetic aspects of 7-dehydrocholesterol reductase and Smith-Lemli-Opitz syndrome. *Biochim. Biophys. Acta.* 1529:340–356.

55. Porter, F. D. 2008. Smith-Lemli-Opitz syndrome: pathogenesis, diagnosis and management. *Eur. J. Hum. Genet.* 16:535–541.

56. Chattopadhyay, A., and Y. D. Paila. 2007. Lipid-protein interactions, regulation and dysfunction of brain cholesterol. *Biochem. Biophys. Res. Commun.* 354:627–633.

57. FitzPatrick, D. R., J. W. Keeling, …, P. T. Clayton. 1998. Clinical phenotype of desmosterolosis. *Am. J. Med. Genet.* 75:145–152.

58. Herman, G. E. 2003. Disorders of cholesterol biosynthesis: prototypic metabolic malformation syndromes. *Hum. Mol. Genet.* 12(Spec No 1):R75–R88.

59. Ranadive, G. N., and A. K. Lala. 1987. Sterol-phospholipid interaction in model membranes: role of C_5-C_6 double bond in cholesterol. *Biochemistry.* 26:2426–2431.

60. Kumari, S. N., G. N. Ranadive, and A. K. Lala. 1982. Growth of a yeast mutant on ring A modified cholesterol derivatives. *Biochim. Biophys. Acta.* 692:441–446.

61. Róg, T., M. Pasenkiewicz-Gierula, …, M. Karttunen. 2007. What happens if cholesterol is made smoother: importance of methyl substituents in cholesterol ring structure on phosphatidylcholine-sterol interaction. *Biophys. J.* 92:3346–3357.

62. Pöyry, S., T. Róg, …, I. Vattulainen. 2008. Significance of cholesterol methyl groups. *J. Phys. Chem. B.* 112:2922–2929.

63. Singh, P., Y. D. Paila, and A. Chattopadhyay. 2007. Differential effects of cholesterol and 7-dehydrocholesterol on the ligand binding activity of the hippocampal serotonin($_{1A}$) receptor: implications in SLOS. *Biochem. Biophys. Res. Commun.* 358:495–499.

64. Paila, Y. D., M. R. V. S. Murty, …, A. Chattopadhyay. 2008. Signaling by the human serotonin($_{1A}$) receptor is impaired in cellular model of Smith-Lemli-Opitz Syndrome. *Biochim. Biophys. Acta.* 1778:1508–1516.

65. Singh, P., R. Saxena, …, A. Chattopadhyay. 2009. Differential effects of cholesterol and desmosterol on the ligand binding function of the hippocampal serotonin($_{1A}$) receptor: implications in desmosterolosis. *Biochim. Biophys. Acta.* 1788:2169–2173.

66. Pucadyil, T. J., and A. Chattopadhyay. 2006. Role of cholesterol in the function and organization of G-protein coupled receptors. *Prog. Lipid Res.* 45:295–333.

67. Paila, Y. D., and A. Chattopadhyay. 2010. Membrane cholesterol in the function and organization of G-protein coupled receptors. *Subcell. Biochem.* 51:439–466.

68. Starke-Peterkovic, T., and R. J. Clarke. 2009. Effect of headgroup on the dipole potential of phospholipid vesicles. *Eur. Biophys. J.* 39:103–110.

69. Duggan, J., G. Jamal, …, H. Harris. 2008. Functional imaging of microdomains in cell membranes. *Eur. Biophys. J.* 37:1279–1289.

70. Robinson, D., N. A. Besley, …, J. D. Hirst. 2011. Water order profiles on phospholipid/cholesterol membrane bilayer surfaces. *J. Comput. Chem.* 32:2613–2618.

71. Hol, W. G. J., P. T. van Duijnen, and H. J. C. Berendsen. 1978. The α-helix dipole and the properties of proteins. *Nature.* 273:443–446.

72. Baron, C. B., and R. F. Coburn. 1984. Comparison of two copper reagents for detection of saturated and unsaturated neutral lipids by charring densitometry. *J. Liq. Chromatogr.* 7:2793–2801.

73. McClare, C. W. F. 1971. An accurate and convenient organic phosphorus assay. *Anal. Biochem.* 39:527–530.

74. Klein, R. A. 1970. The detection of oxidation in liposome preparations. *Biochim. Biophys. Acta.* 210:486–489.

75. MacDonald, R. C., R. I. MacDonald, …, L. R. Hu. 1991. Small-volume extrusion apparatus for preparation of large, unilamellar vesicles. *Biochim. Biophys. Acta.* 1061:297–303.

76. Abrams, F. S., and E. London. 1993. Extension of the parallax analysis of membrane penetration depth to the polar region of model membranes: use of fluorescence quenching by a spin-label attached to the phospholipid polar headgroup. *Biochemistry.* 32:10826–10831.

77. Kremer, J. M. H., M. W. Esker, …, P. H. Wiersema. 1977. Vesicles of variable diameter prepared by a modified injection method. *Biochemistry.* 16:3932–3935.

Supporting Material

Differential Effect of Cholesterol and its Biosynthetic Precursors on Membrane Dipole Potential

Sourav Haldar,[†] Ravi Kumar Kanaparthi,[‡] Anunay Samanta[‡] and Amitabha Chattopadhyay[†]

[†]Centre for Cellular and Molecular Biology, Council of Scientific and Industrial Research, Uppal Road, Hyderabad 500 007, India
[‡]School of Chemistry, University of Hyderabad, Hyderabad 500 046, India

MATERIALS AND METHODS

Materials

1,2-dimyristoyl-*sn*-glycero-3-phosphocholine (DMPC), cholesterol, 7-dehydrocholesterol (7-DHC), desmosterol, ergosterol and coprostanol were obtained from Sigma Chemical Co. (St. Louis, MO). 1-palmitoyl-2-oleoyl-*sn*-glycero-3-phosphocholine (POPC) and 1,2-diarachidonoyl-*sn*-glycero-3-phosphocholine (DAPC), 1,2-dioleoyl-*sn*-glycero-3-phosphocholine (DOPC), 1,2-dioleoyl-*sn*-glycero-3-phosphotempocholine (Tempo-PC), 1-palmitoyl-2-(5-doxyl)stearoyl-*sn*-glycero-3-phosphocholine (5-PC), and 1-palmitoyl-2-(12-doxyl)stearoyl-*sn*-glycero-3-phosphocholine (12-PC), were purchased from Avanti Polar Lipids (Alabaster, AL). 4-(2-(6-(dioctylamino)-2-naphthalenyl)ethyl)-1-(3-sulphopropyl)-pyridinium inner salt (di-8-ANEPPS) was from Molecular Probes (Eugene, OR). The purity of lipids was checked by thin layer chromatography on silica gel precoated plates (Merck) in chloroform/methanol/water (65:35:5, v/v/v) and was found to give only one spot with a phosphate-sensitive spray and on subsequent charring (1). Concentrations of lipids were determined by phosphate assay subsequent to total digestion by perchloric acid (2). DMPC was used as an internal standard. To avoid oxidation of polyunsaturated lipids, the stock solutions of these lipids were stored under argon at -20 °C. Any possible oxidation of polyunsaturated lipids was checked using a spectrophotometric assay (3) and no oxidative damage was detected this way. Water was purified through a Millipore (Bedford, MA) Milli-Q system and used throughout. The concentration of the stock solution of di-8-ANEPPS in methanol was estimated from its molar absorption coefficient of 37,000 $M^{-1}cm^{-1}$ at 498 nm (4).

Sample preparation

All experiments (except depth measurements) were performed using large unilamellar vesicles (LUVs) of 100 nm diameter of POPC (or DAPC) containing increasing concentrations (0-40 mol%) of a given sterol (any one of the following sterols: cholesterol/7-

DHC/desmosterol/ergosterol/coprostanol). All samples contained 1 mol% di-8-ANEPPS. In general, 640 nmol of total lipid (phospholipid and sterol) and 6.4 nmol of di-8-ANEPPS were mixed well and dried under a stream of nitrogen while being warmed gently (~35 °C). After further drying under a high vacuum for at least 3 h, the lipid mixture was hydrated (swelled) by addition of 1.5 mL of 30 mM Tris, 1 mM EDTA, 150 mM sodium chloride, pH 7.2 buffer, and each sample was vortexed for 3 min to uniformly disperse the lipids and form homogeneous multilamellar vesicles. LUVs of 100 nm diameter were prepared by the extrusion technique using an Avestin Liposofast Extruder (Ottawa, Ontario, Canada) as previously described (5). Briefly, the multilamellar vesicles were freeze-thawed five times using liquid nitrogen to ensure solute equilibration between trapped and bulk solutions and then extruded through polycarbonate filters (pore diameter of 100 nm) mounted in an extruder fitted with Hamilton syringes (Hamilton Company, Reno, NV). The samples were subjected to 11 passes through the polycarbonate filters to give the final LUV suspension. Background samples were prepared in the same way except that di-8-ANEPPS was not added to them. The optical density of the samples measured at 420 and 520 nm were less than 0.15 in all cases, which rules out any possibility of scattering artifacts. Samples were incubated in dark for 12 h at room temperature (~23 °C) for equilibration before measuring fluorescence. All experiments were done with multiple sets of samples at room temperature (~23 °C).

Depth measurements using the parallax method

The actual spin (nitroxide) contents of the spin-labeled phospholipids (Tempo-, 5- and 12-PC) were assayed using fluorescence quenching of anthroyloxy-labeled fatty acids (2- and 12-AS) as described previously (6). For depth measurements, liposomes were made by the ethanol injection method (7).   These samples were made by codrying 160 nmol of DOPC containing 10 mol% spin-labeled phospholipid (Tempo-, 5- or 12-PC) and 1 mol% di-8-ANEPPS under a steady stream of nitrogen with gentle warming (~35 °C), followed by further drying under a high vacuum for at least 3 h. The dried lipid film was dissolved in ethanol to give

a final concentration of 40 mM. The ethanolic lipid solution was then injected into 1.5 mL of 30 mM Tris, 1 mM EDTA, 150 mM sodium chloride, pH 7.2 buffer, while vortexing to give a final concentration of 0.11 mM DOPC in buffer. The lipid composition of these samples was DOPC (90%) and 5- (or 12-PC) (10%). Duplicate samples were prepared in each case except for samples lacking the quencher (Tempo-, 5- or 12-PC), for which triplicates were prepared. Background samples lacking di-8-ANEPPS were prepared in all cases, and their fluorescence intensity was subtracted from the respective sample fluorescence intensity. Samples were kept in dark for 12 h before fluorescence measurements.

Table S1

Average Membrane Penetration Depth of di-8-ANEPPS[§]

Spin-labeled PC pair used for quenching analysis	Calculated distance from the bilayer center z_{cF} (Å)	Average z_{cF}[¶] (Å)
Tempo-PC/5-PC	13.9	
		12.2
5-PC/12-PC	10.5	

[§]Depths were calculated from fluorescence quenchings obtained with samples containing 10 mol% of Tempo-, 5- or 12-PC and using Eq. 2. Samples were excited at 498 nm, and emission was collected at 670 nm. The ratio of di-8-ANEPPS to total lipid was 1:100 (mol/mol) and the concentration of di-8-ANEPPS was 1.07 µM in all cases. See Materials and methods for other details.

[¶]The strongest quenching was observed with 5-PC. Since the labels of Tempo-PC and 12-PC quenching were indistinguishable within experimental error (<5% difference in relative fluorescence intensity, *i.e*., $0.95 < F_{12\text{-}PC}/F_{Tempo\text{-}PC} < 1.05$), it was necessary to average z_{cF} values in order to get accurate depth (6).

Supporting References

1. Baron, C. B., and R. F. Coburn. 1984. Comparison of two copper reagents for detection of saturated and unsaturated neutral lipids by charring densitometry. *J. Liq. Chromatogr.* 7:2793-2801.

2. McClare, C. W. F. 1971. An accurate and convenient organic phosphorus assay. *Anal. Biochem.* 39:527-530.

3. Klein, R. A. 1970. The detection of oxidation in liposome preparations. *Biochim. Biophys. Acta* 210:486-489.

4. Le Goff, G., M. F. Vitha, and R. J. Clarke. 2007. Orientational polarisability of lipid membrane surfaces. *Biochim. Biophys. Acta* 1768:562-570.

5. MacDonald, R. C., R. I. MacDonald, B. P. Menco, K. Takeshita, N. K. Subbarao, and L. R. Hu. 1991. Small-volume extrusion apparatus for preparation of large, unilamellar vesicles. *Biochim. Biophys. Acta* 1061:297-303.

6. Abrams, F. S., and E. London. 1993. Extension of the parallax analysis of membrane penetration depth to the polar region of model membranes: use of fluorescence quenching by a spin-label attached to the phospholipid polar headgroup. *Biochemistry* 32:10826-10831.

7. Kremer, J. M. H., M. W. van der Esker, C. Pathmamanoharan, and P. H. Wiersema. 1977. Vesicles of variable diameter prepared by a modified injection method. *Biochemistry* 16:3932-3935.